

---

# Low-Temperature Raman Scattering in $\text{TlGa}_x\text{In}_{1-x}\text{S}_2$ Layered Mixed Crystals: Compositional Dependence of the Mode Frequencies and Line Shapes

N.M. GASANLY\* AND N.S. YUKSEK

Department of Physics, Middle East Technical University, 06531 Ankara, Turkey

(Received June 23, 2005)

The Raman spectra of  $\text{TlGa}_x\text{In}_{1-x}\text{S}_2$  layered mixed crystals were studied for a wide range of composition ( $0 \leq x \leq 1$ ) at  $T = 50$  K. The effect of crystal disorder on the line width broadening of the Raman-active modes are discussed. The asymmetry in the Raman line shape is analyzed for two interlayer and intralayer modes exhibiting one-mode behavior.

PACS numbers: 78.20.-e, 78.30.Hv, 78.30.-j

## 1. Introduction

Layered semiconductors have become increasingly interesting due to their structural properties and potential applications in optoelectronics. Their quasi-two-dimensionality, optical and photoconductive properties, and other features attract investigators in an effort to acquire a better insight into the physics of these compounds. Layered ternary crystals  $\text{TlInS}_2$  and  $\text{TlGaS}_2$  are the anisotropic crystals whose properties have recently become the subject of extensive research [1–8]. A high photosensitivity in the visible range, high birefringence in conjunction with a wide transparency range of 0.5–14  $\mu\text{m}$  make these wide band gap crystals useful for optoelectronic applications [9].

$\text{TlInS}_2$  and  $\text{TlGaS}_2$  belong to the interesting group of layered ternary semiconductors with the chemical formula  $\text{TlBX}_2$ , where  $\text{B} = \text{In}$  or  $\text{Ga}$  and  $\text{X} = \text{S}$  or  $\text{Se}$ . The lattice of  $\text{TlInS}_2$  and  $\text{TlGaS}_2$  consists of strictly periodic two-dimensional layers arranged parallel to the (001) plane. Each successive layer is rotated by right angle with respect to the previous one. Interlayer bonding is formed between

---

\*corresponding author; e-mail: nizami@metu.edu.tr, on leave from Physics Department, Baku State University, Baku, Azerbaijan

Tl and S atoms while the bonding between In (Ga) and S atoms is an intralayer. A view of the crystal structure in the  $ac$ -plane ( $a$  is the axis in the direction  $[110]$ ) is given in Fig. 1, where the layers are also shown. The fundamental structural unit of a layer is the  $\text{In}_4\text{S}_6$  ( $\text{Ga}_4\text{S}_6$ ) adamantane-like units linked together by bridging S atoms. The Tl atoms are in trigonal prismatic voids resulting from the combination of the  $\text{In}_4\text{S}_6$  ( $\text{Ga}_4\text{S}_6$ ) polyhedra into a layer.

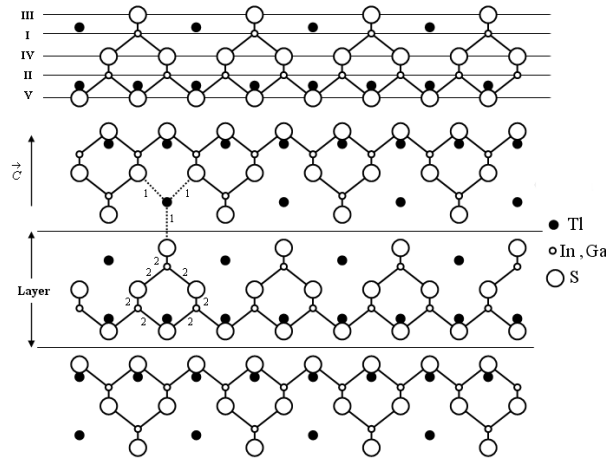


Fig. 1. Projection of the structure in  $\text{TlInS}_2$  and  $\text{TlGaS}_2$  crystals as seen from the  $ac$ -plane. Number 1 shows the interlayer bonding between Tl and S atoms; number 2 shows the intralayer bonding between In (Ga) and S atoms. Numbers from I to V indicate different planes of atoms.

The layer compounds  $\text{TlInS}_2$  and  $\text{TlGaS}_2$  form a series of  $\text{TlGa}_x\text{In}_{1-x}\text{S}_2$  mixed crystals with no restrictions on the concentrations of the components ( $0 \leq x \leq 1$ ) [10]. These mixed crystals are formed when In atoms are substituted with Ga atoms of the same group. In mixed crystals, atoms of the constituent binary compounds are randomly distributed, leading to the fluctuations in the masses and force constants in the neighborhood, and therefore resulting in compositional disorder. Combined with layer stacking faults and various point and line defects, related with less than perfect growth conditions, compositional disorder may affect the vibrational properties of mixed crystals in the form of broadening and asymmetry of phonon modes. Raman spectroscopy is a useful tool to study lattice vibration in mixed crystals. Broadening and asymmetry of phonon lines have been studied in some mixed crystals, such as  $\text{Ga}_{1-x}\text{Al}_x\text{As}$  [11],  $\text{GaAs}_{1-x}\text{P}_x$  and  $\text{In}_x\text{Ga}_{1-x}\text{As}$  [12],  $\text{ZnS}_{1-x}\text{Te}_x$  [13].

The phonon spectra of  $\text{TlGa}_x\text{In}_{1-x}\text{S}_2$  mixed crystals at room temperature have been deduced previously from infrared reflection, Raman, and Brillouin scattering measurements [14–16]. In our previous paper we reported the frequency

dependencies of the Raman-active modes on composition of  $\text{TlGa}_x\text{In}_{1-x}\text{S}_2$  mixed crystals at  $T = 300$  K [14].

The aim of the present work was to study the line shape (full width at half maximum (FWHM) and asymmetry) of optical modes in  $\text{TlGa}_x\text{In}_{1-x}\text{S}_2$  layered mixed crystals using the Raman spectroscopy at  $T = 50$  K. A comparative study between binary compounds and mixed crystals indicates that the anharmonicity increases with increasing compositional disorder in mixed crystals. We discuss the effect of crystal disorder on the FWHM and the asymmetry in the Raman line shape of interlayer and intralayer modes exhibiting one-mode behavior.

## 2. Experimental

Single crystals of  $\text{TlGa}_x\text{In}_{1-x}\text{S}_2$  ( $x = 0, 0.2, 0.4, 0.6, 0.8, 1$ ) were grown by the Bridgman method. The analysis of X-ray diffraction data shows that they crystallize in a monoclinic unit cell. Crystals suitable for measurements were obtained by easy cleavage perpendicular to optical  $c$ -axis. Raman scattering experiments in  $\text{TlGa}_x\text{In}_{1-x}\text{S}_2$  crystals were performed in the backscattering geometry in the frequency range  $10$ – $400$   $\text{cm}^{-1}$ . A  $514.5$  nm line of argon ion laser was used as the exciting light source. The scattered light was analyzed using a double grating spectrometer with a focal length of 1 meter and a cooled GaAs photomultiplier supplied with the usual photon counting electronics. The Raman line positions were determined within an accuracy of  $\pm 0.1$   $\text{cm}^{-1}$ . A closed-cycle helium cryostat was used to cool the crystals from room temperature down to  $50$  K. The temperature was controlled within an accuracy of  $\pm 0.5$  K. In order to avoid sample-heating effects, we have chosen a cylindrical lens to focus the incident beam on the sample.

To achieve a signal-to-noise ratio more than 100, the slit width of the spectrometer was set to  $150$   $\mu\text{m}$ . For slit widths below  $150$   $\mu\text{m}$ , the signal-to-noise ratio is small so that we could not measure the FWHM of some phonon modes with sufficient accuracy. Some phonon lines of  $\text{TlGa}_x\text{In}_{1-x}\text{S}_2$  crystals are so narrow that even with the indicated slit widths, one has to correct for the finite instrument resolution. The width of the response function of the spectrometer was determined by measuring the line width of the laser with the same slit openings as in the Raman experiment. An instrumental line width of  $0.9$   $\text{cm}^{-1}$  was used in the analysis that follows.

## 3. Results and discussion

Figure 2 represents the Raman spectra of  $\text{TlGa}_x\text{In}_{1-x}\text{S}_2$  crystals at  $T = 50$  K. Low-temperature measurements have demonstrated directly that all observed lines are due to one-phonon processes. The phonon spectra of  $\text{TlInS}_2$  and  $\text{TlGaS}_2$  layered crystals exhibit the typical features of vibrational spectra of molecular crystals, namely the presence of low-frequency translational modes of the system consisting of  $\text{In}_4\text{S}_6$  ( $\text{Ga}_4\text{S}_6$ ) units and Tl atoms (interlayer vibrations,

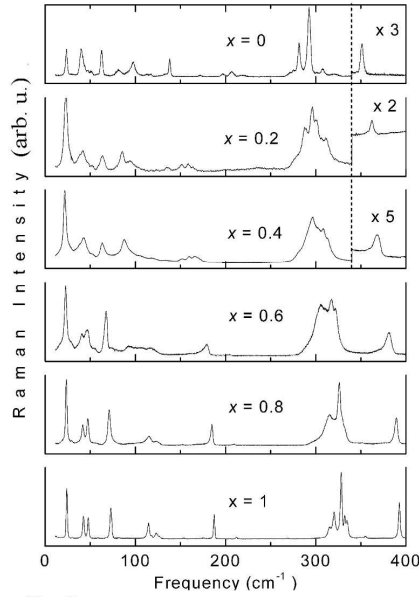


Fig. 2

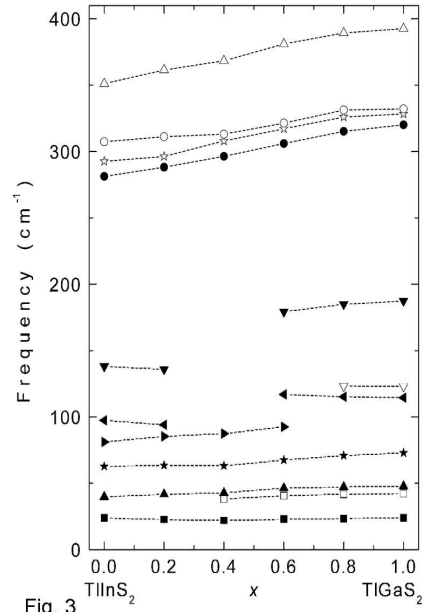


Fig. 3

Fig. 2. Raman spectra of  $\text{TlGa}_x\text{In}_{1-x}\text{S}_2$  mixed crystals at  $T = 50$  K.Fig. 3. Frequency dependencies of the Raman-active modes on composition of  $\text{TlGa}_x\text{In}_{1-x}\text{S}_2$  mixed crystals.

vibrations of Tl atoms, and vibrations of Tl atoms and  $\text{In}_4\text{S}_6$  ( $\text{Ga}_4\text{S}_6$ ) units) and high-frequency “intramolecular” modes of the  $\text{In}_4\text{S}_6$  ( $\text{Ga}_4\text{S}_6$ ) units.

The frequencies and FWHM of the phonons of  $\text{TlGa}_x\text{In}_{1-x}\text{S}_2$  crystals were studied as a function of composition  $x$  (Fig. 2). The shift and broadening of all optical modes with variation of composition are observed. The dependencies of the frequencies of the Raman-active modes on the composition of  $\text{TlGa}_x\text{In}_{1-x}\text{S}_2$  crystals are depicted in Fig. 3. In the low- and high-frequency regions a one-mode behavior is the most typical, while in the middle-frequency region a two-mode behavior is observed. Figure 4 shows the extended low- and high-frequency parts of the Raman spectra of  $\text{TlInS}_2$ ,  $\text{TlGa}_{0.6}\text{In}_{0.4}\text{S}_2$ , and  $\text{TlGaS}_2$  crystals at  $T = 50$  K. A salient feature of the mixed crystal spectra is that anharmonicity due to compositional disorder distorts the phonon line shapes, leading to a tail on the low-energy side. At  $T = 50$  K, anharmonicity is mainly due to compositional disorder-induced anharmonicity.

The mixed crystals cannot have an ideal, perfect periodic lattice. As the Ga composition increases, the disorder effect increases in the mixed crystals  $\text{TlGa}_x\text{In}_{1-x}\text{S}_2$ , and the  $\text{TlInS}_2$  region decreases, while the  $\text{TlGaS}_2$  region increases. This finite periodicity in the mixed crystals relaxes the  $q = 0$  Raman selection rule, thus leading to the broadening and asymmetry of the Raman line shape. We analyzed in detail the compositional dependence of two representatives of the

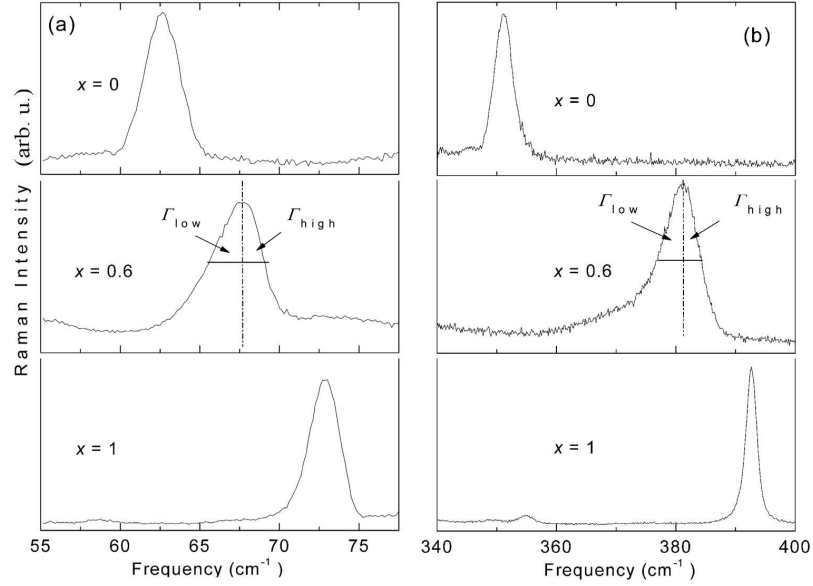


Fig. 4. Extended low-frequency (a) and high-frequency (b) parts of the Raman spectra of  $\text{TlInS}_2$ ,  $\text{TlGa}_x\text{In}_{1-x}\text{S}_2$  for  $x = 0.6$  and  $\text{TlGaS}_2$  crystals at  $T = 50$  K.

Raman-active modes in  $\text{TlGa}_x\text{In}_{1-x}\text{S}_2$  crystals, which exhibit one-mode behavior: low-frequency interlayer mode with frequency varying from  $62.7 \text{ cm}^{-1}$  ( $x = 0$ ) to  $72.9 \text{ cm}^{-1}$  ( $x = 1$ ) and high-frequency intralayer mode with frequency changing from  $351.1 \text{ cm}^{-1}$  ( $x = 0$ ) to  $392.6 \text{ cm}^{-1}$  ( $x = 1$ ). Figure 5 shows the compositional dependencies of the FWHM for these modes. The lifetime of phonons decreases with increasing compositional disorder, making the strongly interacting optical phonons decay into weakly interacting acoustic phonons. The broadening of phonon lines is larger for high-frequency mode as compared to low-frequency mode. As expected, the FWHM dependencies for both modes have maximum in the composition region of  $x = 0.4 \div 0.6$ . Indeed, these compositions of  $\text{TlGa}_x\text{In}_{1-x}\text{S}_2$  mixed crystals correspond to the maximum in substitutional disorder.

Symmetric phonon lines for pure  $\text{TlInS}_2$  and  $\text{TlGaS}_2$  became asymmetric for  $\text{TlGa}_x\text{In}_{1-x}\text{S}_2$  mixed crystals (Figs. 2 and 4). The lower-energy side half-width ( $\Gamma_{\text{low}}$ ) was larger than the high-energy side half-width ( $\Gamma_{\text{high}}$ ). Figure 6 presents the asymmetry ratios ( $\Gamma_{\text{low}}/\Gamma_{\text{high}}$ ) at  $T = 50$  K for two interlayer and intralayer modes exhibiting one-mode behavior. The asymmetry of phonon lines is slightly larger for high-frequency mode as compared to low-frequency mode. The ratios ( $\Gamma_{\text{low}}/\Gamma_{\text{high}}$ ) for both modes show maximum at  $x = 0.4 \div 0.6$ . This indicates that the mixed crystal disorder effect is a main source for the Raman line-shape change as a function of composition.

At this point, it is worthy noting that similar broadening and asymmetry of the phonon lines previously observed in the III–V and II–VI mixed crystals

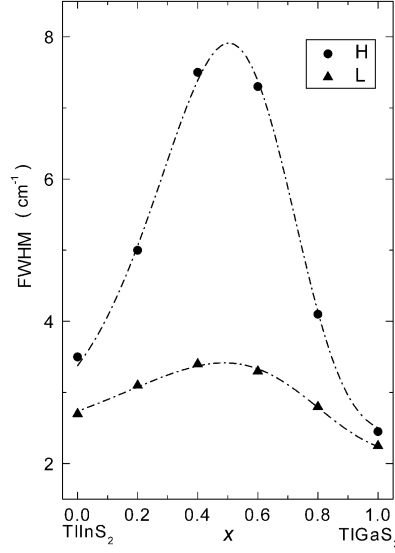


Fig. 5

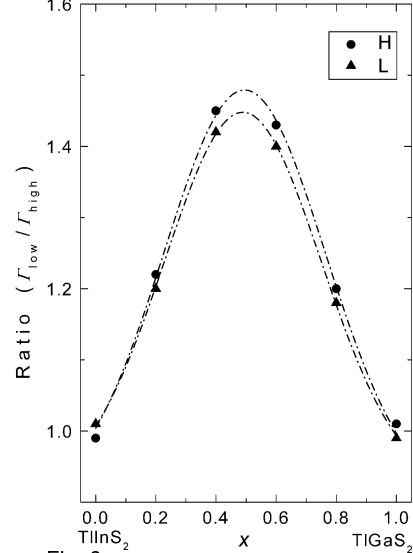


Fig. 6

Fig. 5. Dependencies of the FWHM for low-frequency interlayer mode (L) and high-frequency intralayer (H) mode on composition of  $\text{TlGa}_x\text{In}_{1-x}\text{S}_2$  mixed crystals at  $T = 50$  K. The dash-dotted lines represent guides for the eye.

Fig. 6. Compositional dependence of the ratio  $\Gamma_{\text{low}}/\Gamma_{\text{high}}$  for low-frequency interlayer mode (L) and high-frequency intralayer mode (H) of  $\text{TlGa}_x\text{In}_{1-x}\text{S}_2$  mixed crystals at  $T = 50$  K. The dash-dotted lines represent guides for the eye.

( $\text{Ga}_{1-x}\text{Al}_x\text{As}$  [11],  $\text{GaAs}_{1-x}\text{P}_x$  and  $\text{In}_x\text{Ga}_{1-x}\text{As}$  [12],  $\text{ZnS}_{1-x}\text{Te}_x$  [13]) has been explained using a one-dimensional linear chain model and following the spatial correlation model of Parayanthal and Pollak [17]. Unfortunately, due to the lack of necessary parameters in literature for  $\text{TlInS}_2$  and  $\text{TlGaS}_2$  crystals, we could not apply this model for the explanation of asymmetric broadening of phonon lines in  $\text{TlGa}_x\text{In}_{1-x}\text{S}_2$  mixed crystals.

It is worthy noting that FWHM of corresponding modes for  $\text{TlInS}_2$  crystals were found to be higher than those for  $\text{TlGaS}_2$  crystals (Fig. 5). This may be due to the following factor: atomic radius of the covalently bonded indium (0.144 nm) is larger than that of gallium (0.126 nm) leading to higher probability of defect formation.

#### 4. Conclusions

The Raman spectra for  $\text{TlGa}_x\text{In}_{1-x}\text{S}_2$  layered mixed crystals were investigated for a wide range of composition ( $0 \leq x \leq 1$ ). The FWHM and asymmetry of phonon lines due to crystal disorder were estimated. As expected, both of them have maximum at  $x = 0.4 \div 0.6$ . It was found that the asymmetric broadening of phonon line shapes for a given value of constituent binary compounds in

$TlGa_xIn_{1-x}S_2$  mixed crystals is larger for high-frequency modes as compared to low-frequency modes.

### References

- [1] A. Kato, M. Nishigaki, N. Mamedov, M. Yamazaki, S. Abdullaeva, E. Kerimova, H. Uchiki, S. Iida, *J. Phys. Chem. Solids* **64**, 1713 (2003).
- [2] K.R. Allakhverdiev, N.D. Akhmedzade, T.G. Mammadov, T.S. Mammadov, M.Y. Seidov, *Low Temp. Phys.* **26**, 56 (2000).
- [3] M.P. Haniyas, A.N. Anagnostopoulos, K. Kambas, J. Spyridelis, *Mater. Res. Bull.* **27**, 25 (1992).
- [4] N. Kalkan, J.A. Kalomiros, M.P. Haniyas, A.N. Anagnostopoulos, *Solid State Commun.* **99**, 375 (1996).
- [5] B. Abay, H.S. Guder, H. Efeoglu, H.K. Yogurtcu, *Phys. Status Solidi B* **227**, 469 (2001).
- [6] K.R. Allakhverdiev, N.M. Gasanly, A. Aydinli, *Solid State Commun.* **94**, 777 (1995).
- [7] W. Henkel, H.D. Hochheimer, C. Carlone, A. Werner, S. Ves, H.G. Schnering, *Phys. Rev. B* **26**, 3211 (1982).
- [8] K.R. Allakhverdiev, T.G. Mammadov, R.A. Suleymanov, N.Z. Gasanov, *J. Phys., Condens. Matter* **15**, 1291 (2003).
- [9] K.R. Allakhverdiev, *Solid State Commun.* **111**, 253 (1999).
- [10] N.M. Gasanly, A. Culfaz, H. Ozkan, S. Ellialtioglu, *Cryst. Res. Technol.* **29**, K51 (1994).
- [11] B. Jusserand, J. Sapriel, *Phys. Rev. B* **24**, 7194 (1981).
- [12] C. Ramkumar, K.P. Jain, S.C. Abbi, *Phys. Rev. B* **53**, 13672 (1996).
- [13] Y.M. Yu, D.J. Kim, Y.D. Choi, K.S. Lee, B. O, *J. Appl. Phys.* **95**, 4894 (2004).
- [14] N.M. Gasanly, A.F. Goncharov, N.N. Melnik, A.S. Ragimov, V.I. Tagirov, *Phys. Status Solidi B* **116**, 427 (1983).
- [15] S. Nurov, V.M. Burlakov, E.A. Vinogradov, N.M. Gasanly, B.M. Dzhavadov, *Phys. Status Solidi B* **137**, 21 (1986).
- [16] N.M. Gasanly, B.G. Akinoglu, S. Ellialtioglu, R. Laiho, A.E. Bakhyshev, *Physica B* **192**, 371 (1993).
- [17] P. Parayanthal, F.H. Pollak, *Phys. Rev. Lett.* **52**, 1822 (1984).